This is to certify that the

thesis entitled

MATHEMATICAL MODELLING OF ISOTOPE
EXTRACTION FROM SKELETAL
MUSCLE VASCULATURE

presented by

Mark Alan Holmes

has been accepted towards fulfillment
of the requirements for

M.S. degree in Chemical Engineering

Major professor

Date November 10, 1978

O-7639

MATHEMATICAL MODELLING OF ISOTOPE EXTRACTION FROM SKELETAL MUSCLE VASCULATURE

By

Mark Alan Holmes

A THESIS

Submitted to
Michigan State University
in partial fulfillment of the requirements
for the degree of

MASTER OF SCIENCE

Department of Chemical Engineering

1978

ABSTRACT

MATHEMATICAL MODELLING OF ISOTOPE
EXTRACTION FROM SKELETAL
MUSCLE VASCULATURE

By

Mark Alan Holmes

The selection of parameter estimates and bounds in a mathematical modelling technique was examined. A technique was developed to analyze washout curves from extraction studies on the canine gracilius muscle. The mathematical models employed simulated vascular beds with and without shunt channels. With the proper selection of initial parameter estimates and bounds, the simulation technique adequately represented the experimental data.

The two-path model (with shunt) describes the experimental data more accurately than the single path model (no shunt). However, from the analysis of the data available to date, it is not clear if the skeletal muscle vasculature contains shunt vessels.

TO THE LORD,

who got it done, and

TO KAREN,

who helped.

ACKNOWLEDGEMENTS

The author would like to express his appreciation to his academic advisor, Dr. Donald K. Anderson, for his guidance and assistance. He would also like to express his gratitude to Dr. Jerry B. Scott, Michael L. Goodnight, and Gregory A. Goslow for their advice and cooperation during the course of this research. Finally, he would like to thank his wife, Karen, for all of her support and assistance.

The financial support of the National Institute of Health and the Michigan Heart Association is gratefully acknowledged.

TABLE OF CONTENTS

LIST OF TABLES

LIST OF FIGURES

NOMENCLATURE

a	In one-path model, fraction of the total system volume in the main flow stream, dimensionless. In two-path model, the fraction of stream 1 volume in the main stream, dimensionless.
B	In the one-path model, ratio of tracer exchange rate to the main stream flow, dimensionless. In two-path model, ratio of tracer exchange rate to stream 1 flow, dimensionless.
C	Concentration, mc/ml.
D	Computer parameter, equivalent to B
E(t)	Exit-age-distribution function as a function of time, sec^{-1}.
E(θ)	Exit-age-distribution function as a function of dimensionless time, dimensionless.
f	In two-path model, fraction of total flow going to stream 1, dimensionless.
G	Constant, see equation 35, dimensionless.
I(t)	Internal-age-distribution function as a function time, sec^{-1}.
I(θ)	Internal-age-distribution function as a function of dimensionless time, dimensionless.
K	Constant, see equation 15, dimensionless.
M	In two-path model, number of stirred tanks in stream 2.
N	In one-path model, number of stirred tanks in series. In two-path model, number of stirred tanks in stream 1.
Q	Constant, see equation 16, dimensionless.
R	Constant, see equation 15, dimensionless.

t	Time, minutes; seconds.
$\bar{t}$	Mean residence time, minutes; seconds.
v	Blood flow rate, ml/min; ml/min/100 gm.
V	Volume, ml; ml/100 gm.
α	In two-path model, the ratio of the mean residence time in stream 2 to the mean residence time in stream 1, dimensionless.
β	Constant, see equation 21, dimensionless.
γ	Computer parameter equivalent to "a".
ε	Fraction of total volume in the plug flow section, dimensionless.
η	In the two-path model, the ratio of the volume of a tank in stream 2 to the volume of a tank in stream 1, dimensionless.
θ	Dimensionless time.
Θ	Variable, see equation 12, dimensionless.
$\Lambda(t)$	Intensity function as a function of time, sec^{-1}.
$\Lambda(\theta)$	Intensity function as a function of dimensionless time, dimensionless.
ϕ	Fraction of tracer recovered, dimensionless.

Subscripts

B	Blood
D	Diffusible
I	Injected
ND	Nondiffusible
T	Total system
tubing	tubing
1	Function 1 or stream 1
2	Function 2 or stream 2

INTRODUCTION

The goal of this research was to continue a study on the vasculature of skeletal muscle. In particular, this work involved further development of computer modelling techniques, initially presented by M. R. Borghi (6), to be used in the analysis of radioisotope pulse injection data obtained from canine gracilis muscles.

The equations used in the computer simulations were derived from modelling techniques used extensively in the engineering field. A discussion of the work of other investigators, in both the engineering and physiological areas, is presented in the Background section. A description of the models and equations used is also presented.

The data which were analyzed were obtained from experimental procedures described in detail by M. L. Goodnight (12). In brief, the gracilis muscle of a mongrel dog was isolated in situ, leaving only one artery leading to the muscle and one vein draining it. Radiolabelled compounds were injected as a bolus into the artery feeding the muscle, and samples of venous blood were taken serially and analyzed.

The experimental data from the washout studies were converted to age-distribution curves and analyzed. The primary analytical method consisted of fitting the experimental results with computer generated curves of mathematical models.

Discussion of the results and conclusions of this research is contained in the final section.

BACKGROUND

The Capillary Bed

Flow through a vascular bed can best be described using the schematic diagram in Figure 1. Blood enters through the artery (A) which branches into arterioles (a) which branch into capillaries (c). Exchange of nutrients and metabolic wastes between the blood tissue occurs at the capillary level. The capillaries drain into venules (v) which, in turn, empty into veins (V).

Vessel diameters range from 600 - 1,000 microns for terminal arteries and veins, 20 - 30 microns for the arterioles and venules, and 8 - 12 microns for true capillaries. True capillaries can also be distinguished from the larger vessels by their walls, since they contain only endothelial cells, while the walls of the larger vessels also contain smooth muscle and collagen fibers.

Actually, the capillary network is far more complex than is indicated in Figure 1. For example, flow in a given capillary can, and does, change directions as indicated in Figure 2. A more detailed description of the capillary and its function can be found in Mountcastle (20, pp. 984-991).

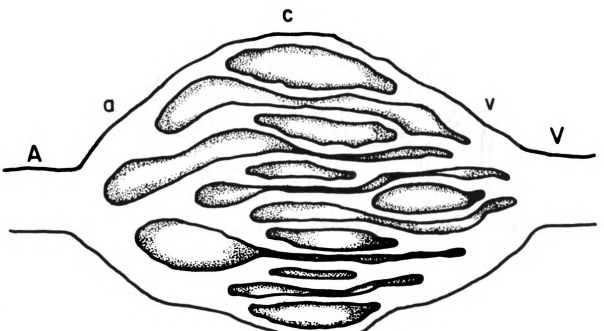

Figure 1.-- Schematic diagram of vascular bed.

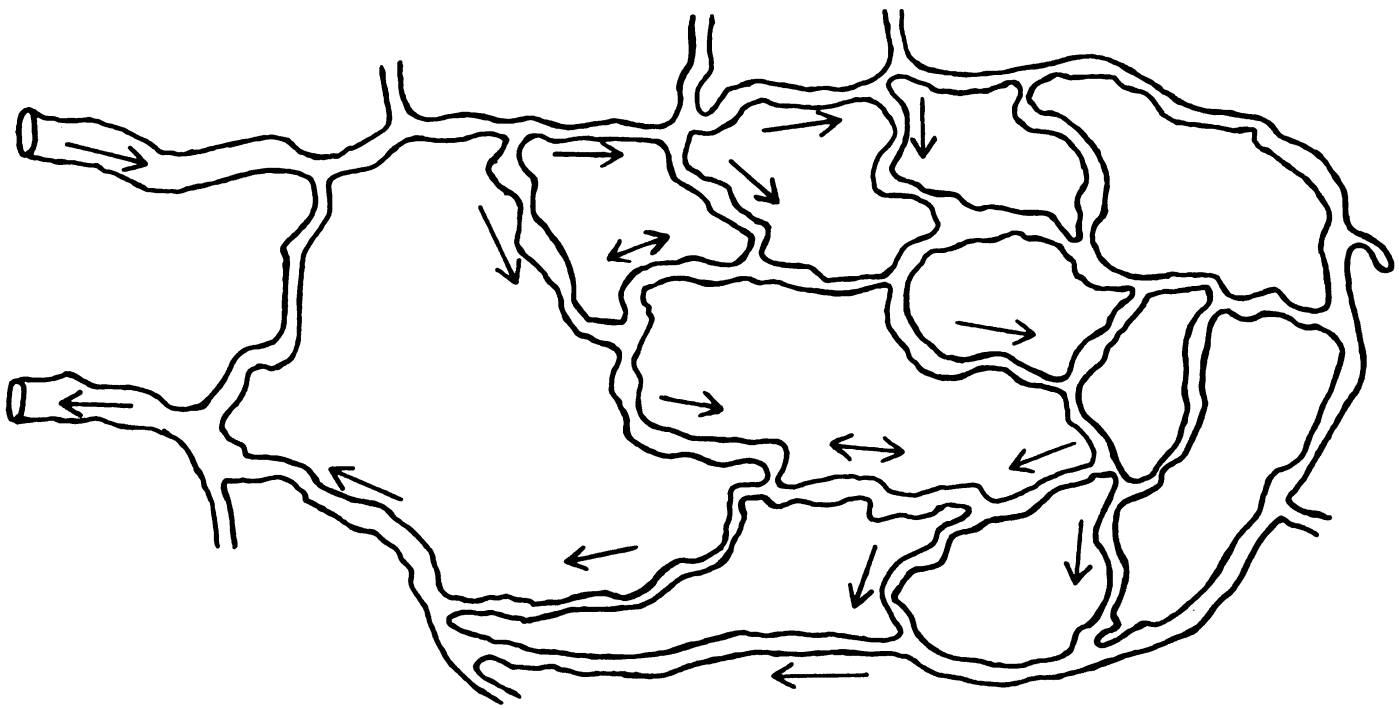

→ Blood Flow Direction

Figure 2.--Schematic diagram of a capillary network with change in flow direction. Adapted from Borghi (6, p. 2).

Work of Other Investigators

The work done by other investigators can roughly be divided into two groups: 1) those studying skeletal blood flow and, 2) those developing the modelling techniques.

Skeletal Muscle Studies

Two important contributors to research on blood flow through skeletal muscle are J. J. Friedman (8-11) and E. M. Renkin (22-25). Both have conducted indicator dilution studies on skeletal muscles, and each has proposed a theory to explain his observations.

Friedman supports the hypothesis that skeletal muscle blood flow is best described as a flow limited, two-path system, where one path (referred to as the nutritive path) supplies oxygen and nutrients to the tissue, and the second path (or nonnutritive path) shunts excess blood around or past the capillary bed, as in an arteriovenous anastomosis. No anatomical anastomoses have been identified in skeletal muscle. However, a physiological shunt, consisting of preferential pathways, may exist (see 6, Figure 1). In this system, the preferential pathways would act to shunt excess blood flow by the capillary bed, while the true capillaries would supply the nutritive needs of the muscle.

According to Renkin's theory, nutrient supply to the skeletal muscle is permeability limited, with the possibility of one or more paths. In this study, only the one-path model was considered. The use of this model is consistent with Renkin's definition, since the additional stream(s) serve(s) as a source of additional capillaries for increased blood flow (22, 23).

A third investigator, C. H. Baker (1-4, 19), has also been working in the analysis of blood flow through skeletal muscle vascular beds. Utilizing the parallel path model, he has attempted to calculate the volumes associated with radio-labelled red blood cell, albumin, and rubidium flow paths.

Population Balance Studies

In the engineering field, the work of Danckwerts (7) in 1953 is considered the forerunner of present tracer washout modelling techniques. In the area of physiology, indicator dilution studies were used as early as 1928 by Hamilton (13, 14), with detailed derivations by Zierler (18, 26-29). It is interesting to note that Zierler went through an analysis of vascular beds very similar to the one Danckwerts did with reactor beds one year earlier. The work in the physiological area has been further developed by investigators such as Martin and Yudelivich (17), while Levenspiel (16),

Bischoff (5), and others (see citations in 15) have developed the modelling techniques formalized by Danckwerts in the engineering field.

The research described in this thesis involves applying engineering models to the study of the skeletal muscle vasculature.

MODELS, EQUATIONS, AND COMPUTER PROGRAMS

Age-Distribution Functions

The equations used in this study are from a group of functions called age-distribution functions, which have been described previously (7, 21). The equations, or functions, describe the residence time of fluid elements in a theoretical, idealized system, which can hopefully be related to the physical system being examined. In engineering applications, this would include reaction mixtures flowing through reactor beds. In this biological study the equations are used to describe the residence time of blood in the muscle capillary bed. Three of the age-distribution functions are described below.

Internal-Age-Distribution Function

The internal-age-distribution function, I(t), is the age distribution inside the system, and has the units: fraction of ages per unit time. The "age" of any element is defined as the time, t, the element has spent in the system. From this, the fraction of elements in the vessel with ages between t and t+dt is given by I(t)dt. The function is normalized, which leads to

$$\int_0^\infty I(t)dt = 1 \tag{1}$$

Exit-Age-Distribution Function

The exit-age-distribution function, E(t), is defined as the residence time distribution of the stream leaving the system. It is the distribution, or frequency, of fluid elements of a given age in the exit stream. It has the same units as I(t), and the fraction of the exit stream with ages between t and t+dt is given by E(t)dt. This function is also normalized which leads to

$$\int_0^\infty E(t)dt = 1 \tag{2}$$

The exit-age-distribution function is related to the internal-age-distribution function by

$$E(t) = -\bar{t}\,\frac{d}{dt}I(t) \tag{3}$$

Intensity Function

The intensity function, Λ, is defined as the fraction of fluid in the system of age t that will leave at a time between t and t+dt. It is related to the other two functions by

$$\Lambda(t) = \frac{1}{\bar{t}}\,\frac{E(t)}{I(t)} \tag{4}$$

The functions can be expressed in dimensionless form, where θ, the dimensionless time, is defined as

$$\theta = \frac{t}{\bar{t}} \tag{5}$$

and $\bar{t}$, the mean resident time, is defined as

$$\bar{t} = {}_0\int^{\infty} tE(t)dt \tag{6}$$

The dimensionless age-distribution functions then become

$$E(\theta) = \bar{t}E(t) \tag{7}$$

$$I(\theta) = \bar{t}I(t) \tag{8}$$

$$\Lambda(\theta) = \bar{t}\ (t) = \frac{E(\theta)}{I(\theta)} \tag{9}$$

More detailed derivations of the functions can be found in the texts by Levenspiel (16) or Himmelblau and Bischoff (15).

The Models and Equations

Borghi (6, pp. 11-57) developed four models to describe the age-distribution functions for diffusible and non-diffusible tracers expected from the theories proposed by Renkin and Friedman. The models used consist of arrangements of ideal stirred and/or ideal plug flow vessels. In an ideal stirred tank, the entire contents of the vessel are completely mixed and uniform.

An ideal plug flow reactor is one in which there is complete mixing perpendicular to the direction of flow, but no mixing or diffusion along the direction of flow.

Renkin Models

As mentioned earlier, the Renkin hypothesis concerning blood flow is represented by a single pathway. For the non-diffusible tracer, the model consists of a plug flow vessel, (PF) followed by a series of equal volumed stirred tanks (ST) as shown in Figure 3. The age-distribution function is given by

$$E(\theta) = \begin{cases} 0 & \text{for } \theta \leq \varepsilon \\ \dfrac{N^N \quad \Theta^{N-1}}{\Gamma(N)(1-\varepsilon)} \exp(-N\,\Theta) & \text{for } \theta \geq \varepsilon \end{cases} \tag{10}$$

where

$$\varepsilon = \frac{V_{PF}}{V_T} \tag{11}$$

$$\Theta = \frac{\theta - \varepsilon}{1 - \varepsilon} \tag{12}$$

The model for the diffusible tracer is similar to the model for the nondiffusible tracer. The diffusion model consists of the same plug flow tank and series of stirred tanks with the addition of a diffusion tank (DT).

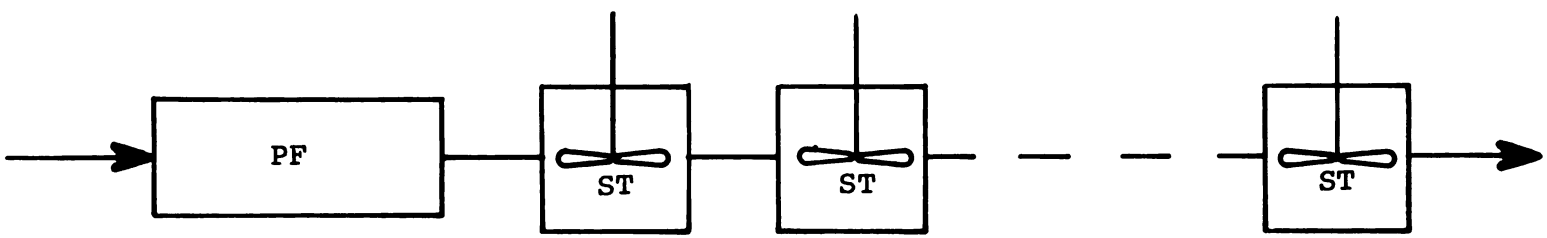

PF - Plug Flow Tank
ST - Stirred Tank

Figure 3.-- Schematic diagram of the one-channel, nondiffusible tracer model (Renkin).

The diffusion tank is used to represent the diffusion of tracer in and out of the interstitial space, and consists of a stirred tank which receives flow from, and sends flow to, the last stirred tank in the series as indicated in Figure 4. The dimensionless age-distribution function for the single-path diffusion model is give by

$$E(\theta) = \frac{K_1 Q}{(1-\varepsilon)} \left[\exp(-Q\,\Theta) \sum_{i=1}^{N-1} \frac{\left[(1+aR_1)Q\Theta\right]^{N-i-1}}{(N-i-1)!} - \exp(aQR_1\Theta) \right]$$

$$- \frac{K_2 Q}{(1-\varepsilon)} \left[\exp(-Q\,\Theta) \sum_{i=1}^{N-1} \frac{\left[(1+aR_2)Q\Theta\right]^{N-i-1}}{(N-i-1)!} - \exp(aQR_2\Theta) \right] \tag{13}$$

for $\theta \geq \varepsilon$ and 0 for $\theta \leq \varepsilon$, where

$$R_2^1 = \frac{1-a+B}{2a(1-a)} \left[-1 \pm \sqrt{1 - \frac{4aB(1-a)}{(1-a+B)^2}} \right] \tag{14}$$

$$K_2^1 = \frac{R_2^1 + B/(1-a)}{(1 + aR_2^1)^{N-1} (R_2 - R_1)} \tag{15}$$

$$Q = \frac{aN - a + 1}{a} \tag{16}$$

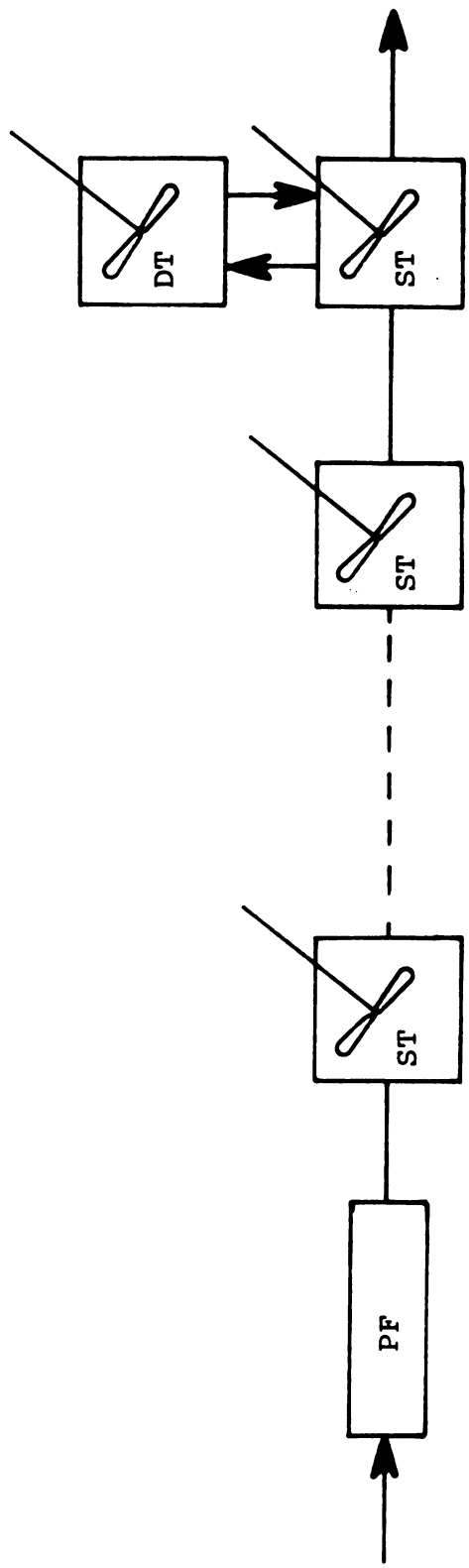

PF - Plug Flow tank
ST - Stirred Tank
DT - Diffusion Tank

Figure 4.-- Schematic diagram of the one-channel, diffusible tracer model (Renkin).

Friedman Models

The Friedman model is represented by a two-channel flow path. The nondiffusible tracer path is represented by a plug flow vessel followed by two parallel streams of stirred tanks, designated as streams 1 and 2. Stream 1 has N tanks, each having a volume V_1, and stream 2 has M tanks, each having volume V_2. A schematic diagram of the model is presented in Figure 5. The dimensionless exit-age-distribution function for this model is given by

$$E(\vartheta) = f \frac{(N\beta)^N \Theta^{N-1}}{\Gamma(N) \quad (1-\varepsilon)} \exp(-N\beta\Theta) + (1-f) \frac{(M\beta/\alpha)^M \Theta^{M-1}}{\Gamma(M) \quad (1-\varepsilon)} \exp\left[-\frac{M\beta}{\alpha}\Theta\right] \tag{17}$$

for $\theta \geq \varepsilon$, and 0 for $\theta \leq \varepsilon$, where

$$\varepsilon = \frac{V_{PF}}{V_T} \tag{18}$$

$$\Theta = \frac{\theta-\varepsilon}{1-\varepsilon} \tag{19}$$

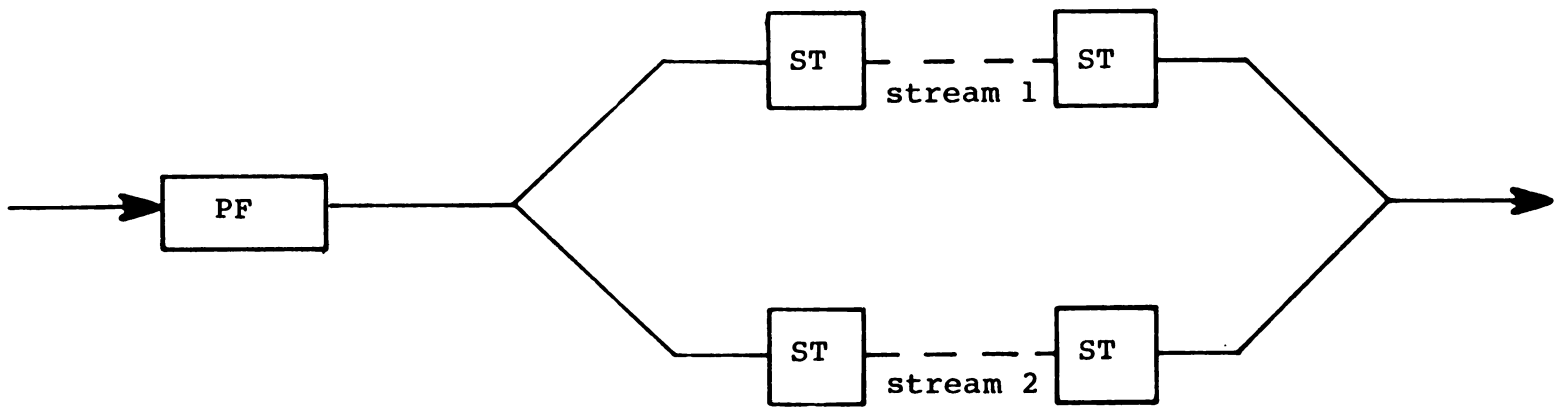

Figure 5.--Schematic diagram of the two-channel, nondiffusible tracer model (Friedman).

$$\alpha = \frac{fMV_2}{(1-f)NV_1} \tag{20}$$

$$\beta = f+(1-f)\alpha \tag{21}$$

For the diffusible tracer, a diffusion tank (DT) is added to stream 1, as indicated in Figure 6.

$$E(\theta) = \frac{fQK_1\beta}{(1-\epsilon)}\left[\exp(-Q\beta\theta)\sum_{i=1}^{N-1}\frac{\left[Q\beta(1+aR_1)\theta\right]^{N-i-1}}{(N-i-1)!} - \exp(aQR_1\beta\theta)\right]$$

$$- \frac{fQK_2\beta}{(1-\epsilon)}\left[\exp(-Q\beta\theta)\sum_{i=1}^{N-1}\frac{\left[Q\beta(1+aR_2)\theta\right]^{N-i-1}}{(N-i-1)!} - \exp(aQR_2\beta\theta)\right]$$

$$+ \frac{(1-f)\,\theta^{M-1}}{(1-\epsilon)\,(M-1)!}\left[\frac{M\beta}{\alpha}\right]^{M}\exp-\left[\frac{M\beta}{\alpha}\theta\right] \tag{22}$$

for $\theta \geq \epsilon$ and 0 for $\theta \leq \epsilon$, where

$$\alpha = \frac{faMV_2}{(1-f)\,(aN-a+1)V_1} \tag{23}$$

and ϵ, θ, R_2^1, K_2^1, β, and Q are as defined earlier.

Computer Program Modifications

The computer programs used in this research were versions of Fortran IV programs written by Borghi (6, p. 100). Four major modifications were made in the programs. First, subroutine Area was eliminated because the values of $\bar{t}$ calculated in the subroutine were

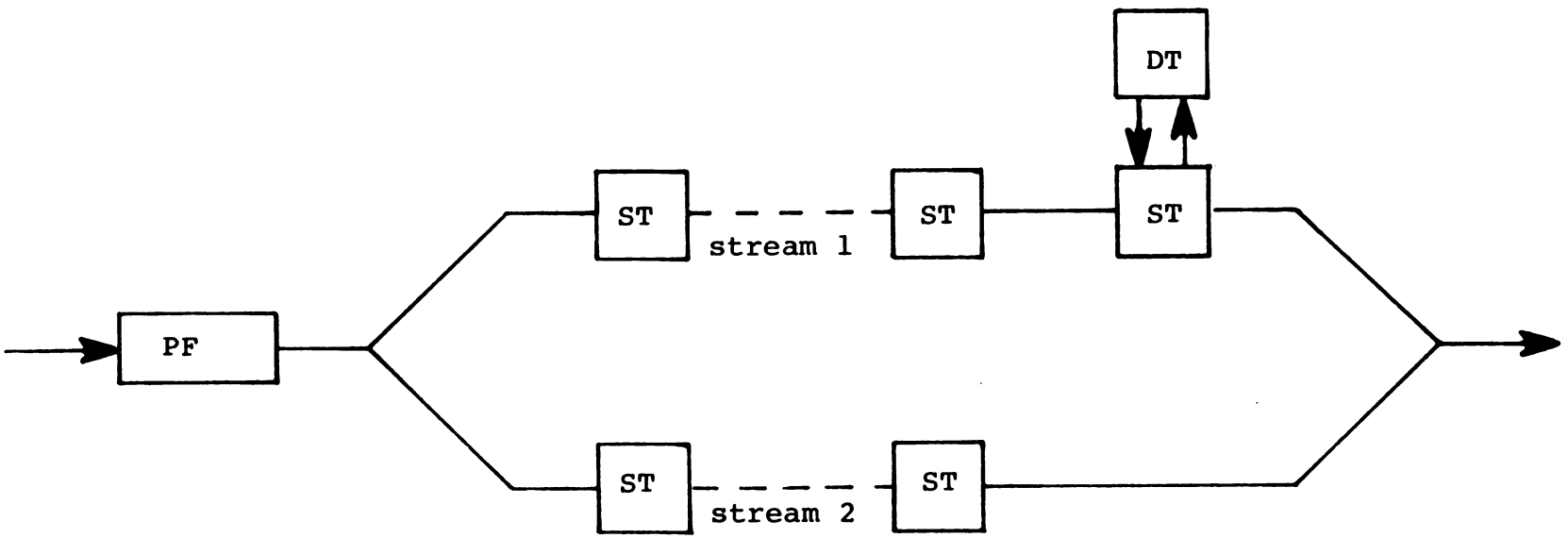

PF - Plug Flow Tank
ST - Stirred Tank
DT - Diffusion Tank

Figure 6.--Schematic diagram of the two-channel, diffusible tracer model (Friedman).

unreasonable, often greater than 200 seconds. Secondly, the channel volume calculations were found to be incorrect and were replaced.

Thirdly, nonzero values of $E(\theta)$ were given by the model subroutines for values of $\theta \leq \varepsilon$, which is incorrect. Alterations were made to account for the lower values. Finally, the main program and model subroutines were modified so the subroutines could be called up by calling either Model (used by the curve fitting program) or by calling the individual subroutine name (Series, Renkin, or Friedman; used with other programs). This eliminated the need to alter the subroutines' names each time they were used with a different program.

The modified programs are presented in the Appendix. The optimization portion of the program (subroutine Opt) and the plotting subroutine (Plotter) were not altered, and are not presented.

METHODS AND RESULTS

Surgical Procedure

Mongrel dogs weighing approximately 20 kg were anesthetized with sodium pentobarbitol (30 mg/kg). The gracilis muscle (M, see Figure 7) was surgically approached from the medial aspect of the hind limb, and all vessels except the primary artery and vein (indicated by A and V, respectively) were ligated. An essentially nonpulsatile, perfusion pump (P in Figure 7) was used to pump blood from the contralateral femoral artery to the primary artery. Venous blood from the muscle flowed through a sampling valve (SV), which, when activated, flushed intermittent, serial blood samples of equal volume into collection vials (CV).

During the washout studies, it was desirable that the blood not be returned to the dog in order to eliminate the possibility of tracer recirculation. Therefore, during the washout periods, the blood leaving the sampling value was discarded, and dextran-70 was infused into the contralateral femoral vein at approximately the same rate as blood was lost. Between studies, the blood was returned to the dog via the contralateral femoral vein.

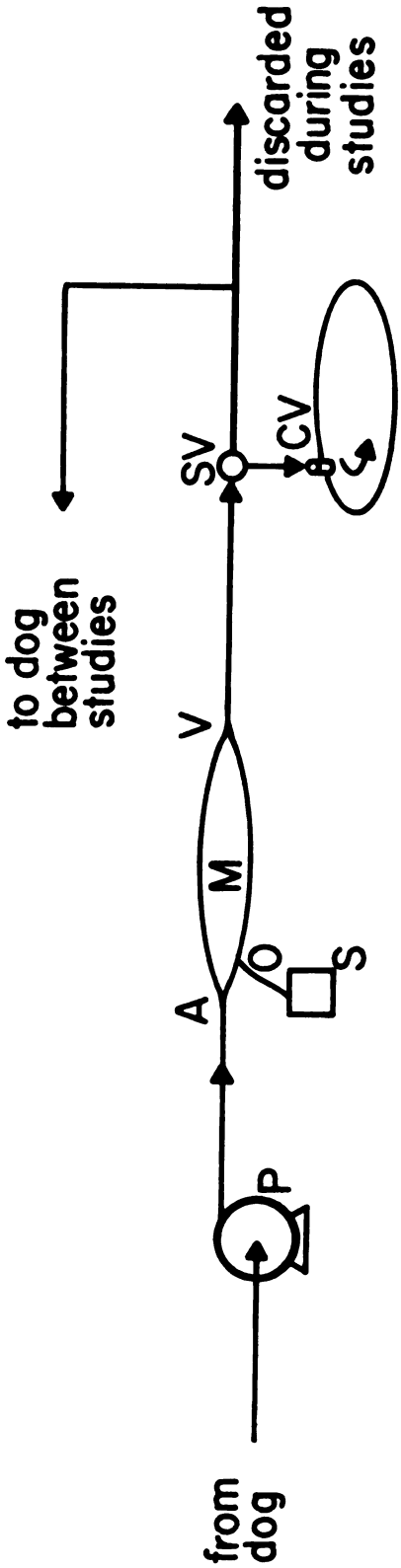

Figure 7.--Schematic diagram of experimental procedure.

The muscle was tied at its origin and insertion to eliminate any collateral flow, and the obturator nerve (O) was cut and connected to an electronic stimulator (S). Systemic arterial, perfusion, and venous pressures were monitored using pressure transducers, and recorded on a strip chart. Timing signals from the sampling value controller were also recorded.

Experimental Procedure

Sucrose, labelled with C^{14}, and H^3 tagged dextran (MW 82,400) were used as the diffusible and nondiffusible tracers, respectively. One bolus of a mixture of the tracers in saline solution was injected into the primary artery during each of the three washout studies performed on each dog. As a control, the first study was done without stimulation. The second injection was made immediately after electrical stimulation of the muscle (6v, 6 cps, 1.6 msec, for 30 seconds). The third injection was made after five minutes of histamine infusion (10 mg/ml at 0.5 ml/min). The histamine infusion continued throughout the sampling period.

The blood samples were bleached with percholoric acid and hydrogen peroxide, then counted in a liquid scintillation counter. The counts obtained from the scintillation counter were converted to tracer

concentrations and the concentrations were then converted to exit-age parameters utilizing the formula

$$E(t) = \frac{C_B v}{C_I V_I} \qquad (24)$$

where C_B is the tracer concentration in the blood, v is the blood flow rate, C_I is the tracer concentration injected, and V_I is the volume of tracer solution injected. A more detailed explanation of the experimental procedure is presented by Goodnight (12).

Results

Much of the experimental data could not be fully analyzed due to low tracer recoveries. In many instances, dextran recovery at the completion of a washout study was less than 70%. This was especially true for the stimulation experiments. Further complications arose from the need to use dextran washout parameters in analyzing the corresponding sucrose data. The poor quality of the dextran data, therefore, often led to the discarding of otherwise usable sucrose data.

Five sets of experimental data were selected for analysis: Four dextran washout studies and one sucrose washout study. Four of the sets of data are from control experiments, and one is from a stimulation experiment. Values for the experimental parameters are given in Table 1, and the data is presented in Tables 2-6.

Table 1.--Experimental Parameters

Data Set*	Blood Flow (ml/min)	Muscle Weight (gms)	Sample Spacing (seconds)	Estimated Tracer Recovery** %
10 - C - D	9.6	74.80	6.280	98.6
10 - C - S	9.6	74.80	6.280	85.5
10 - St - D	9.6	74.80	6.280	96.4
11 - C - D	16.8	79.98	5.600	88.8
24 - C - D	15.9	85.50	2.125	100.0

*Dog number - Experiment (C = control, ST = stimulation - Tracer (D = dextran, S = sucrose)
**To last data point

Table 2.--Data Set 10 - C - D

Time (seconds)	E(t) ($seconds^{-1}$)	Time (seconds)	E(t) ($seconds^{-1}$)
2.00	.00000	102.48	.00103
8.28	.00000	108.76	.00087
14.56	.00003	115.04	.00084
20.84	.00288	121.32	.00076
27.12	.03385	127.60	.00064
33.40	.03982	133.88	.00059
39.68	.02563	146.44	.00045
45.96	.01460	152.72	.00039
52.24	.00986	159.00	.00035
58.52	.00585	165.28	.00028
64.80	.00401	171.56	.00029
71.08	.00303	177.84	.00028
77.36	.00249	184.12	.00025
83.64	.00179	190.40	.00023
89.92	.00137	196.68	.00021
96.20	.00122	202.96	.00019

Table 3.--Data Set 10 - C - S

Time (seconds)	E(t) ($seconds^{-1}$)	Time (seconds)	E(t) ($seconds^{-1}$)
2.00	.00000	102.48	.00132
8.28	.00000	108.76	.00116
14.56	.00003	115.04	.00106
20.84	.00243	121.32	.00096
27.12	.02684	127.60	.00089
33.40	.03069	133.88	.00082
39.68	.01827	146.44	.00068
45.96	.01065	152.72	.00065
52.24	.00713	159.00	.00062
58.52	.00500	165.28	.00061
64.80	.00373	171.56	.00057
71.08	.00299	177.84	.00055
77.36	.00245	184.12	.00052
83.64	.00202	190.40	.00047
89.92	.00172	196.68	.00046
96.20	.00152	202.96	.00045

Table 4.--Data Set 10 - St - D

Time (seconds)	E(t) ($seconds^{-1}$)	Time (seconds)	E(t) ($seconds^{-1}$)
2.00	.00000	108.76	.00108
8.28	.00003	115.04	.00095
14.56	.00007	121.32	.00081
20.84	.00193	127.60	.00064
27.12	.02188	133.88	.00058
33.40	.04498	140.16	.00049
39.68	.02953	146.44	.00053
45.96	.01502	152.72	.00036
58.52	.00579	159.00	.00030
64.80	.00416	165.28	.00027
71.08	.00291	171.56	.00025
77.36	.00217	177.84	.00021
83.64	.00173	184.12	.00019
89.92	.00170	190.40	.00017
96.20	.00136	196.68	.00016
102.48	.00127		

Table 5.--Data Set 11 - C - D

Time (seconds)	E(t) ($seconds^{-1}$)	Time (seconds)	E(t) ($seconds^{-1}$)
4.00	.00000	172.00	.00027
9.60	.00000	177.60	.00023
15.20	.01684	183.20	.00023
20.80	.05498	188.80	.00019
26.40	.03658	194.40	.00020
32.00	.01348	200.00	.00024
37.60	.00871	205.60	.00018
43.20	.00531	211.20	.00019
48.80	.00294	214.20	.00019
54.40	.00259	219.80	.00020
60.00	.00201	225.40	.00015
65.60	.00149	231.00	.00015
71.20	.00113	236.60	.00017
76.80	.00099	242.20	.00014
82.40	.00092	247.80	.00013
88.00	.00088	253.40	.00011
93.60	.00083	259.00	.00012
99.20	.00063	264.60	.00013
104.80	.00055	270.20	.00012
110.40	.00049	275.80	.00012
116.00	.00039	281.40	.00012
121.60	.00037	287.00	.00018
127.20	.00042	292.60	.00010
132.80	.00028	298.20	.00010
138.40	.00031	303.80	.00009
144.00	.00025	309.40	.00009
149.60	.00024	315.00	.00009
155.20	.00022	320.60	.00009
160.80	.00024	326.20	.00010
166.40	.00019	331.80	.00014

Table 6.--Data Set 24 - C - D

Time (seconds)	E(t) ($seconds^{-1}$)	Time (seconds)	E(t) ($seconds^{-1}$)
2.68	.00000	45.13	.00440
4.75	.00000	47.25	.00411
6.88	.00000	49.38	.00373
9.00	.00211	51.50	.00303
11.13	.01451	53.63	.00273
13.25	.05200	55.75	.00309
15.38	.07486	57.88	.00298
17.50	.08238	60.00	.00232
19.63	.04792	62.13	.00220
21.75	.04520	64.25	.00195
23.88	.02928	66.38	.00176
26.00	.02354	68.50	.00211
28.13	.01774	70.63	.00179
30.25	.01726	72.75	.00164
32.38	.01218	74.88	.00176
34.50	.00913	77.00	.00152
36.63	.00865	79.13	.00154
38.75	.00719	81.25	.00151
40.88	.00655	83.38	.00146
43.00	.00529		

METHODS OF ANALYSIS

Preliminary Calculations

Calculation of Tracer Recovery

The tracer recovery, ϕ, is obtained by integration of the exit-age-distribution function. In equation form, the fraction of tracer recovered to time t is given by

$$\phi(t) = {}_0\int^t E(t)dt \tag{25}$$

Since all of the tracer should eventually be washed out to the tissue,

$$\phi(\infty) = {}_0\int^\infty E(t)dt = 1 \tag{26}$$

Estimation of the tracer recovered during an experiment was made using Euler's estimation of the integral. The dextran tracer concentration in the venous blood was sufficiently low by the end of most experiments to justify the conclusion that all of the tracer that could be washed out of the tissue had been extracted. Extrapolation of the curves usually accounted for less than an additional 5-10% of the tracer recovery. Therefore, dextran data sets with less than 90% recovery by the last data point were not analyzed. The dextran

data set from the control experiment of dog number 11 was included, however, to illustrate the problem encountered with low tracer recovery.

Mean Residence Time Calculation

The equation for the mean residence time, $\bar{t}$, was presented in Section II. (p. 11). The integration of the exit-age-distribution data was done graphically, as numerical techniques often gave unreasonable values due to the methods used to estimate the tail portion of the curve. The mean residence times for the sucrose data are only approximations. The tail portion of that data set made a more exact determination of $\bar{t}$ impossible. However, the data are adequate for illustration of the analytical techniques.

Data and Weighting Factors

For curve fitting purposes, the data beyond $\theta = 2$ or 3 could not be considered reliable (15, p. 72), and were not used in the analysis. To compensate for the large number of data points in the tail portion of the washout curves, the peak data point was weighted 10 times heavier than the other points. Once the initial optimization was completed, any necessary alterations in the curve fit could be made by using a weighting scheme to emphasize the portion of the curve where the improvement was desired.

Parameter Estimations

Plug Flow Volume Calculations

In order to obtain an estimate of the plug flow volume, V_{PF}, blood flow in the tubing from the injection site to the muscle, and from the muscle to the sampling valve, was assumed to be plug flow in nature. The tubing volume used in the experiments, as calculated from the tubing diamter and length, was 1.9 ± .4 ml.

The total system volume, V_T, is related to $\bar{t}$ and blood flow, v, by

$$V_T = v\bar{t} \tag{27}$$

From this, ε, the fraction of the total volume in the plug flow section, is given by

$$\varepsilon = \frac{V_{PF}}{V_T} \simeq \frac{V_{tubing}}{V_T} \simeq \frac{1.9}{v\bar{t}} \tag{28}$$

The value of ε could not be defined precisely since the primary artery and vein might also show plug flow characteristics. However, the calculated value was used as the first estimate of ε in the curve fitting optimization.

Tank Number Parameters

Borghi (6) found that the two-stream model gave a better curve fit than the one-stream model, since the one-stream model could not simultaneously fit both the peak and the tail portions of the data adequately. Similar results were found in this study, as shown in Figure 8. When the two-path model was used, the lower limit on the number of tanks in each stream was set at 3.0 to avoid anomalies in the mathematics, and the upper limit set at 50.0. Initial estimates for N and M were taken as 3.0 and 15.0, respectively.

Fractional Flow Parameter

The fraction of the total fluid flow in stream 1, f, was allowed to range from 0.0 to 1.0. The initial parameter estimate was defined as 0.4, as the optimized values were usually less than 0.5.

Ratio of Tank Volumes

The ratio of a tank volume from stream 2 to a tank volume from stream 1, η, was allowed to range from 0.0 to 10.0, with an initial estimate of 0.2. The final, optimized values for this parameter were less than 0.5.

Diffusible Model Parameters

For the two-path diffusible model, the values for ε, f, N, M, and η were defined by the corresponding

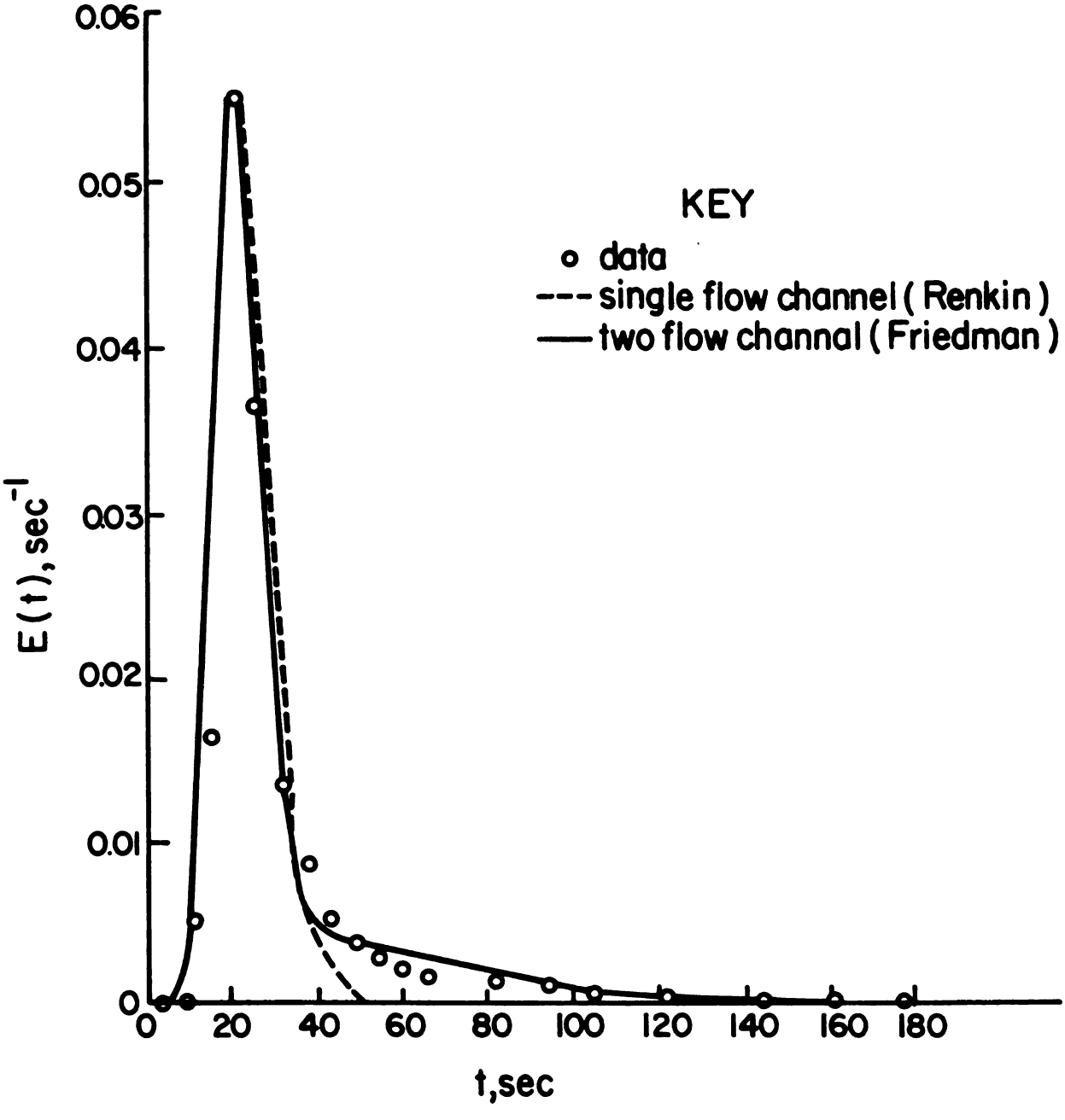

Figure 8. Comparison of one- and two-channel models to data set 11 - C - D.

nondiffusible optimization. The values for f, N, M, and η were the same in the diffusible case as in the nondiffusible case, and ε_D was defined by

$$\varepsilon_D = \frac{\varepsilon_{ND} \quad \bar{t}_{ND}}{\bar{t}_D}$$

It should be noted that stream 1 was defined as the nutritive (diffusion) stream, and stream 2 was defined as the shunt (nondiffusion) stream when the two-channel, diffusible tracer model was used. Therefore, with this model, f was the fraction of the total blood flow going to the nutritive stream, and N was the number of tanks in the nutritive stream. Likewise, η was the ratio of the volume of a tank in the shunt stream to the volume of a tank in the nutritive stream.

The value of "a" (referred to as γ in the computer programs), the fraction of the total stream 1 volume which was present in the main stream, was calculated using the equation

$$a = \frac{G\bar{t}_{ND}}{(G - 1)\bar{t}_{ND} + \bar{t}_D}$$

where

$$G = \frac{1 - ND}{1 + \frac{M\eta}{N}}$$

B (referred to as D in the computer programs) was defined as the ratio of flow to and from the diffusion tank to the main stream flow. The value of B was allowed to range from 0.0 to 100.0, with an initial estimate of 0.01. Since this was the only parameter being optimized in this model, the initial estimate was not as critical as in the case of the nondiffusibile tracer model parameters. Curve fitting of the sucrose data was done in which each of the streams from the corresponding dextran optimization was defined as the nutritive stream. The best fits for each configuration were compared, and the optimum fit was selected.

The Modelled Data

The mean residence times, optimized parameter values, and the sum of the squared residuals for each of the sets of modelled data are presented in Table 7. The calculated values of α and β, from equations 20 and 21, respectively, for the nondiffusible tracer model are also included in Table 7 to facilitate the use of equation (d) from Himmelblau's text (15, p. 74). The calculated physical parameters are presented in Table 8. Comparisons of the computer derived curves and the experimental data are presented in Figures 9-13.

Table 7.--Computer Derived Parameter Values

Data Set*	Parameters								Sum of Squared Residuals		
	$\bar{t}$ (sec)	ε	f	N	M	γ	D	η		α	β
10 - C - D	48.0	.387	.24	3.0	4.0			.568	.252	.24	.42
10 - C - S	55.0	.350	.38	3.0	3.0			.385	.172	.24	.53
10 - C - S	50.0	.371	.76	4.0	3.0	.86	.19	1.760	.391		
10 - St - D	46.0	.220	.35	3.0	15.0			.173	.053	.47	.65
10 - C - D	27.0	.118	.48	3.0	17.4			.132	.108	.71	.85
24 - C - D	22.25	.317	.53	3.0	12.0			.115	.154	.52	.77

*See Table 1 for explanation

Table 8.--Calculated Physical Parameters

Data Set *	Plug Flow Volume	Stream 1 (diffusion stream)**			Stream 2 (shunt stream)**	
		Capillary Volume	Blood Flow	Interstitial Space Volume	Capillary Volume	Blood Flow
	ml/100 gm	ml/100 gm	ml/min/100 gm	ml/100 gm	ml/100 gm	ml/min/100 gm
10 - C - D	4.0	3.6	3.1		2.7	9.7
10 - C - S[1]	4.1	5.5	4.8		2.1	8.0
10 - C - S[2]	4.0	2.7	9.7	.43	3.6	3.1
10 - St - D	2.2	4.1	4.5		3.6	8.3
11 - C - D	1.1	4.9	10.3		3.5	11.0
24 - C - D	2.2	3.2	9.8		1.5	8.8

*See Table 1 for explanation
**If applicable
[1]Nondiffusible tracer model, $\bar{t}$ = 55.0
[2]Diffusible tracer model, $\bar{t}$ = 50.0

Figure 9.--Comparison of computer derived curve and data set 10 - C - D.

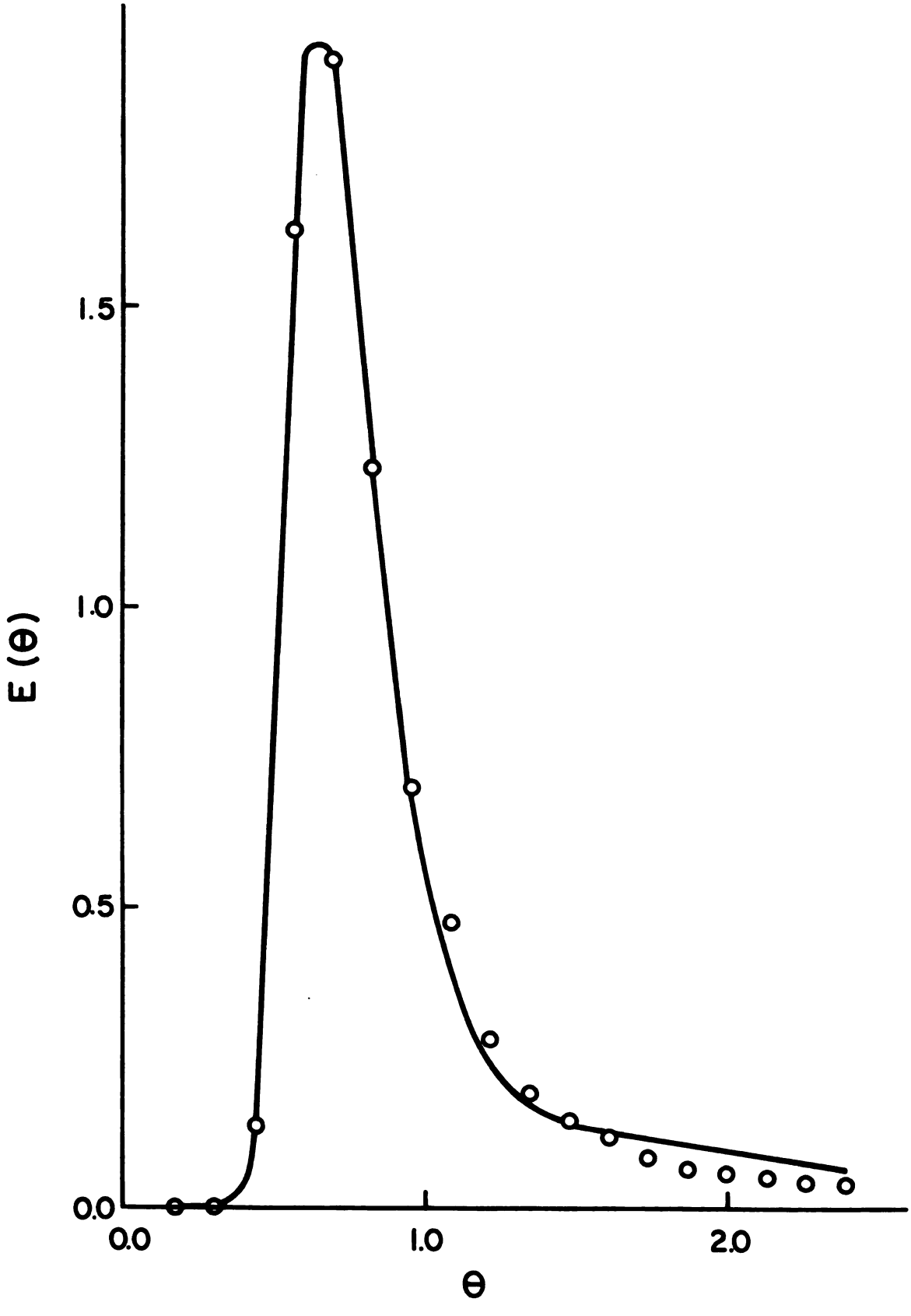
E (θ)
1.5
1.0
0.5
0.0
0.0
1.0
2.0
θ

Figure 10.--Comparison of computer derived curves and data set 10 - C - S.

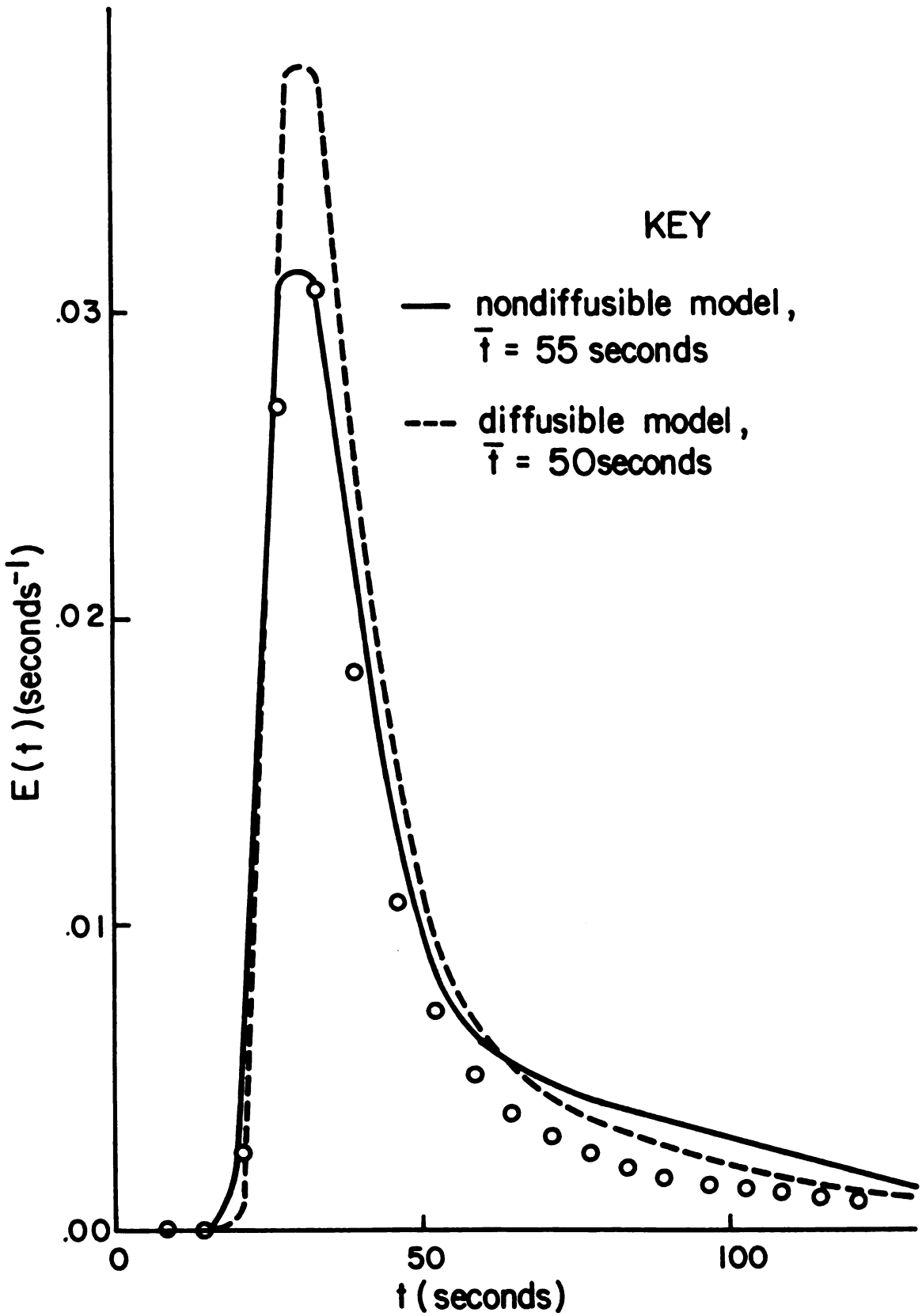
KEY
nondiffusible model, $\bar{t}$ = 55 seconds
diffusible model, $\bar{t}$ = 50seconds
E(t)(seconds^{-1})
.03
.02
.01
.00
0
50
100
t (seconds)

Figure 11.--Comparison of computer derived curve and data set 10 - St - D.

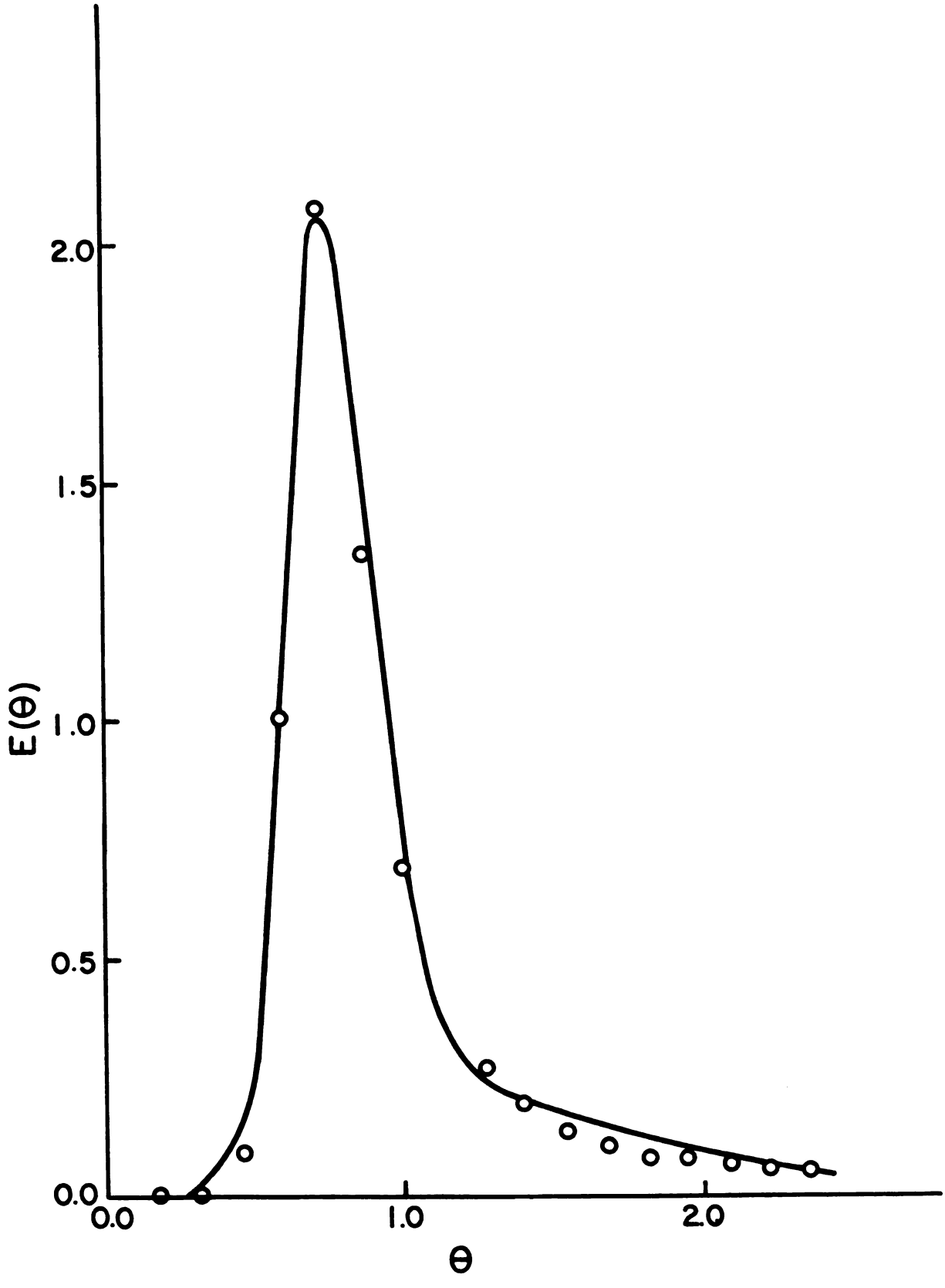
2.0
1.5
1.0
0.5
0.0
E(θ)
0.0
1.0
2.0
θ

Figure 12.--Comparison of computer derived curve and data set 11 - C - D.

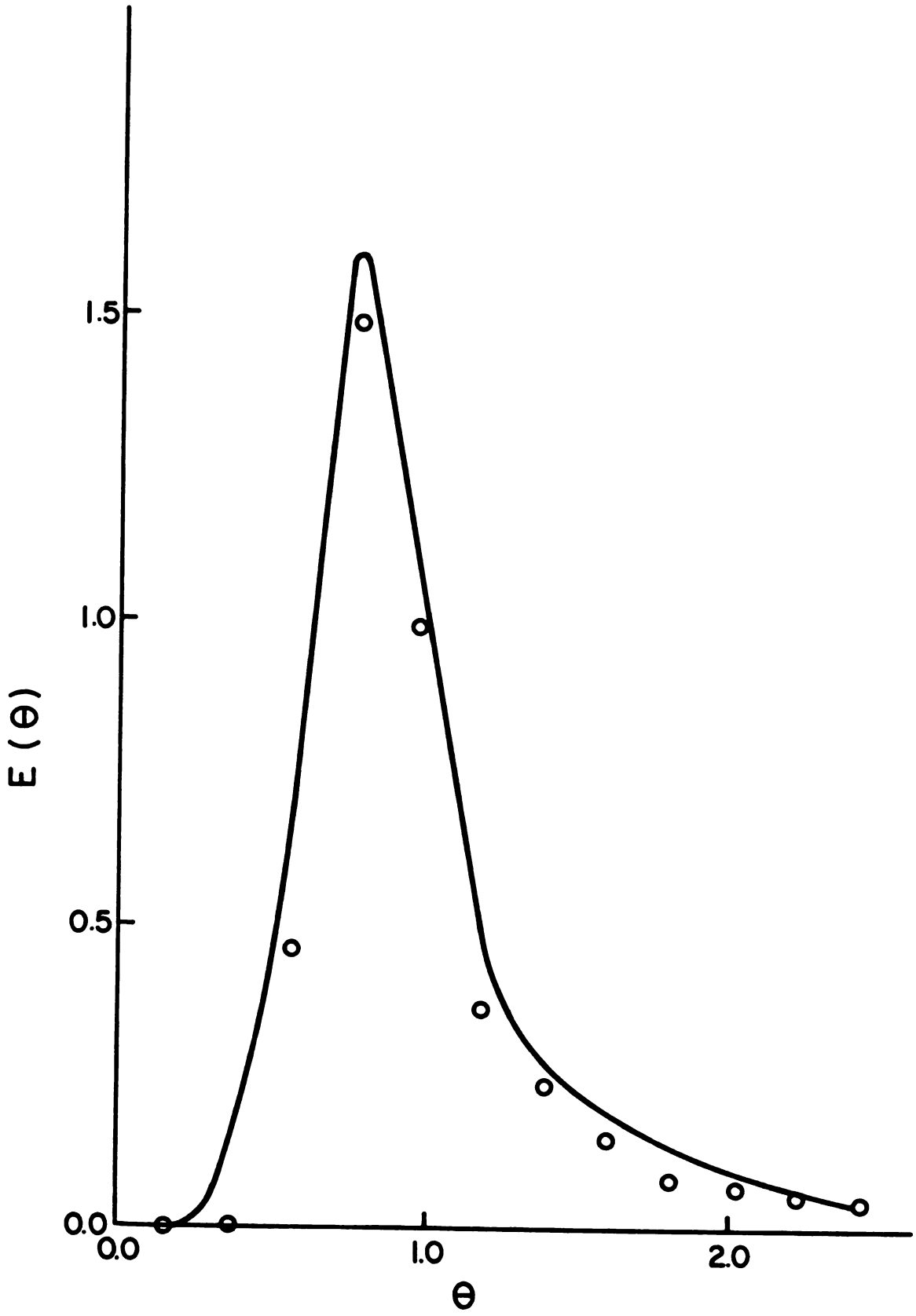
1.5
1.0
0.5
0.0
E (θ)
0.0
1.0
2.0
θ

Figure 13.--Comparison of computer derived curve and data set 24 - C - D.

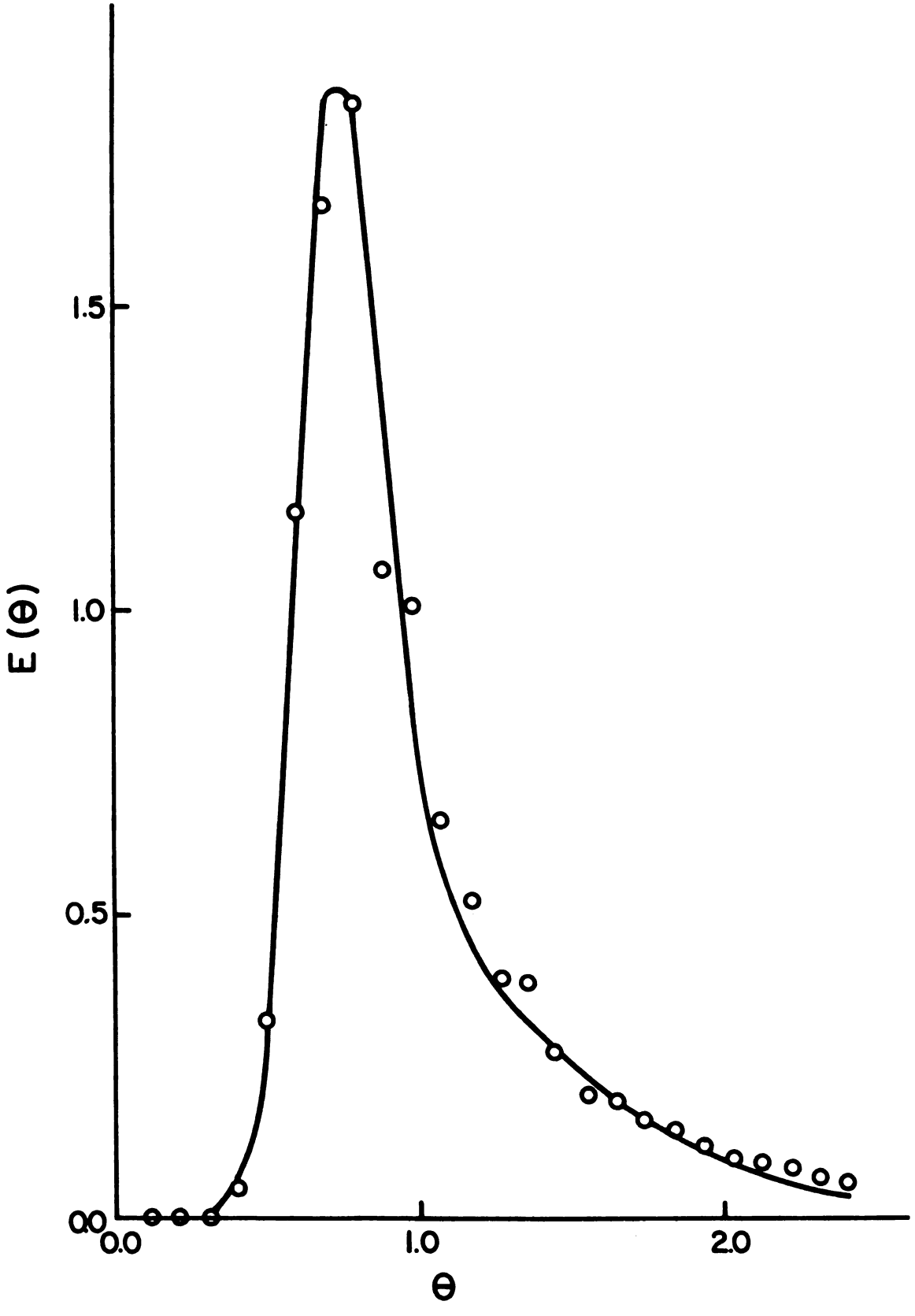
E (θ)
1.5
1.0
0.5
0.0
0.0
1.0
2.0
θ

DISCUSSION

Experimental Procedure

Equipment Modifications

Equipment modifications improved the quality of the data obtained from the experiments. The use of a chromatographic sample injection valve (12) eliminated the dead space problems encountered by Borghi (6). The use of a new timing device decreased the sampling interval from 4-6 seconds to 1-3 seconds. This increased the number of data points on the peak portion of the washout curve, and decreased the possibility of missing the peak portion of the curve, which occasionally occurred with the previous timer.

Tracers

The primary difficulty encountered in this study was the poor quality of the dextran washout data. Over 60% of the control and stimulation experiments had dextran recoveries less than 70%, and in almost 40% of the experiments, dextran recovery was less than 50%. In contrast, only 20% of the control and stimulation sucrose recoveries were less than 70%. The sampling period for each experiment exceeded 250 seconds, allowing adequate

time for the complete extraction of the nondiffusible tracer (the blood recirculation time in the normal canine is approximatley 30 seconds).

As can be seen in Figure 12, the low tracer recovery in data sets 11 - C - D made adequate fitting of the data impossible. The computer derived curve is above the data at all points. This problem also occurred when attempts were made to model the data from experiment 10 - C - S (recovery 85.5%).

The low level of detected dextran recovery is believed to be due to the loss of the tritium through an exchange reaction. The possibility of replacing the dextran tracer with I^{125} labelled albumin is being examined in the continuation of the project.

Plug Flow Tubing Assumption

One washout study was conducted on blood flowing through tubing, without the muscle. The normalized data collected in that experiment is compared to the non-diffusible tracer data from dog number 24 in Figure 14. Additional washout studies on blood flow through the tubing should be conducted to test the assumption of plug flow in the tubing. If that assumption is incorrect, it would be necessary to replace the plug flow section of the model with a series of stirred tanks (Figure 15).

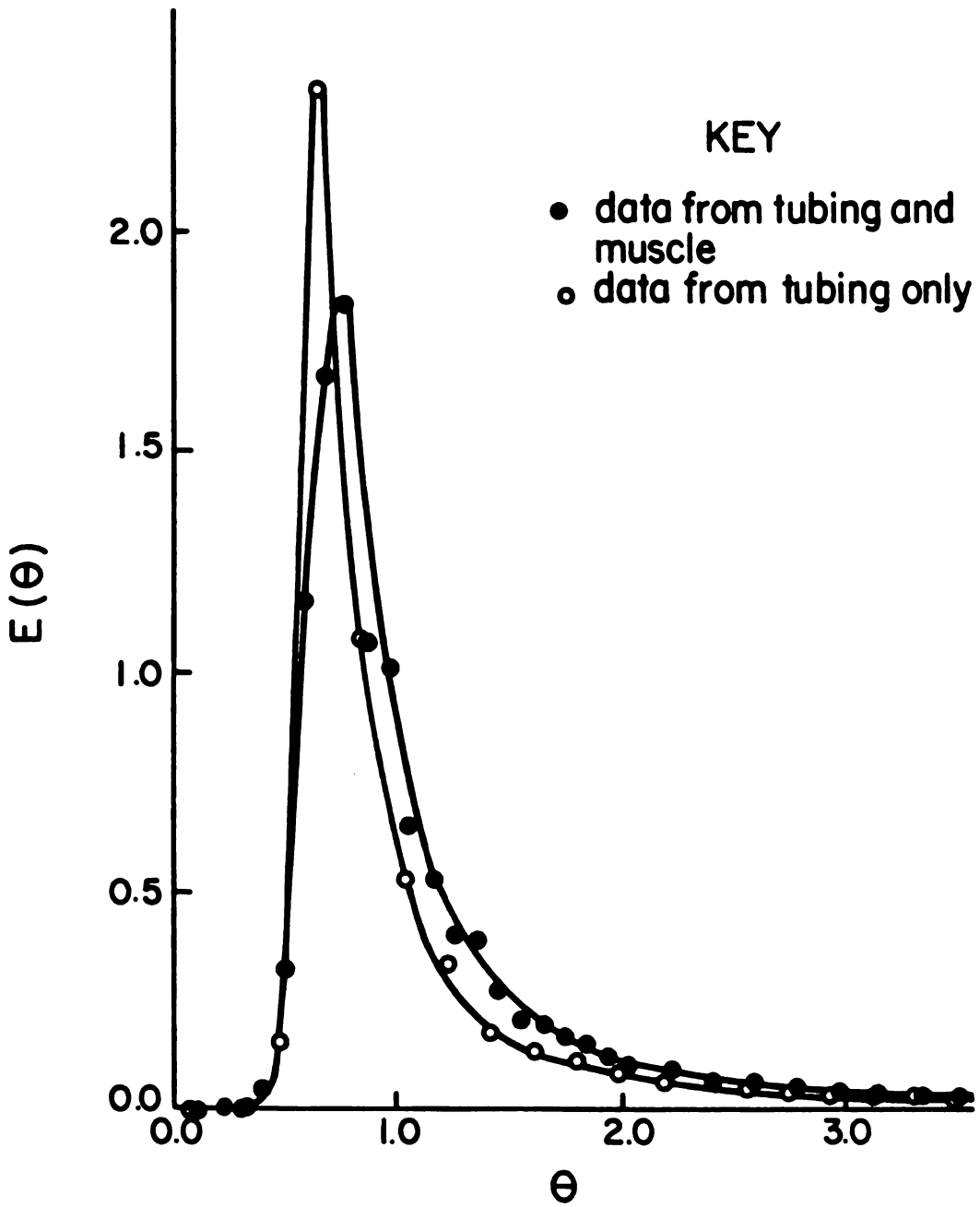

Figure 14.--Comparison of normalized washout data from tubing and muscle (data set 24 - C - D) and tubing only.

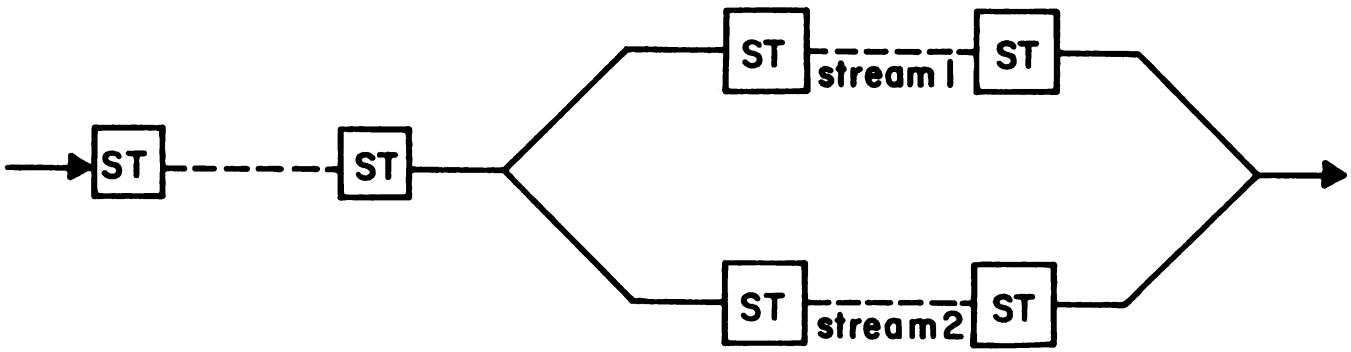

Figure 15.--Schematic diagram of the two-channel, nondiffusible tracer model with stirred tanks (ST) replacing the plug flow section.

Modelling Techniques

Curve Fitting Capabilities

With the exceptions of data sets 10 - C - S and 11 - C - D, the modelling techniques adequately represented the data (see Figures 9, 11 and 13). The primary requirements for the optimization techniques were high tracer recovery and the selection of reasonable initial parameter estimates and bounds.

With the use of randomly selected parameters, the curve fitting program often "optimized" to curves which did not reasonably represent the data. The problem was especially pronounced when the data peak was not preferentially weighted. The large number of data points in the tail overemphasized that portion of the curve. In addition, if multiple maxima were present in the optimization scheme, random initial parameter selection may have caused the program to optimize around the incorrect maximum.

Because of the uncertainty of the mean residence time calculations for the sucrose data set, that set was optimized using several different values for $\bar{t}$. The best fits for the nondiffusible and diffusible models were presented (see Figure 10). As mentioned earlier, the low tracer recovery for this data set hindered the optimization efforts. However, since only one parameter is optimized with the diffusible tracer

model, the optimization technique is expected to perform adequately with more reliable data.

Other Age-Distribution Functions

The possibility of replacing the exit-age-distribution function, E(t), in the optimization technique with one of the other-age distribution functions was considered. The information obtained from the internal-age-distribution function, I(t), is similar to that obtained from E(t), and there was no significant advantage to using the former. The intensity function, $\Lambda(t)$, is helpful for detecting bypassing or stagnation in a flow system. The appearance of two or more maxima in the $\Lambda(t)$ curve indicates the presence of nonuniform flow. However, the intensity function is not as useful as the other two functions in quantifying the effect (15, p. 73).

Conclusions

Theory Comparison

It is not possible to draw any definite conclusions from the data available at this time concerning which of the two hypotheses (Renkin's or Friedman's) is correct. The need for a two-path system to represent the data supports Friedman's theory, as does the high sucrose exchange rate which is inconsistent with the permeability limited system described in Renkin's theory.

However, analysis of more reliable data than are presently available will be required to resolve the question.

With the proper selection of initial parameter estimates and bounds, the modelling techniques described above can be expected to perform adequately.

Suggestions

The utilization of the sampling valve and control timer, developed by other investigators working on the project, has significantly improved the quality of the data. Replacing the radiolabelled dextran tracer and testing the assumption of plug flow in the tubing are areas which should be addressed in the continuation of the skeletal muscle microcirculation research.

APPENDIX

COMPUTER PROGRAMS

```
      PROGRAM MAIN(INPUT,OUTPUT)
      DIMENSION BNDLW(10), B(10), BNDUP(10), CHMAX(10), DEL(10)
      DIMENSION Y(60), F(60), IX(60,5), IAH(6), SYM(4)
      COMMON/IWT/IWT
      COMMON/SYMBOL/SYMBOL,SYM
      COMMON X(60,5), G(60,5), W(60), IGOR, FRAC
      DATA SYM,FACTOR,IAH/1HD,1HC,1H0,1H0,40.0001,0,0 ,0,-0,-0,-0/
      CALL SYSTEMC(115,IAH)
C
C     BNDLW, B, BNDUP ARE THE LOWER BOUND, INITIAL GUESS AND UPPER BOUND
C      OF THE PARAMETER RESPECTIVELY.
C     CHMAX IS THE MAXIMUM CHANGE THAT CAN OCCUR IN ANY ITERATION.
C     DEL IS THE INCREMENT TO BE USED IN DERIVATIVE CALCULATIONS.
C     X IS THE VARIABLE ARRAY AND Y IS THE OBSERVATION ARRAY.
C     IWT DETERMINES WHETHER THE OBSERVATIONS ARE NORMALIZED.
C      IF ZERO THEY ARE, AND IF NONZERO THEY ARE NOT.
C     NOB IS THE NUMBER OF OBSERVATIONS.
C     NPAR IS THE NUMBER OF VARIABLE PARAMETERS TO BE FITTED.
C     NVAR IS THE TOTAL NUMBER OF DEPENDENT AND INDEPENDENT VARIABLES IN
C      THE FUNCTION.
C     ITMAX IS THE MAXIMUM NUMBER OF ITERATIONS TO BE PERFORMED BY LS.
C     LISTS DETERMINES THE OUTPUT PRINTED BY LS.
C     W IS A WEIGHTING FACTOR GIVEN TO EACH DATA POINT.
C     FPM IS THE TOTAL FLOW RATE IN ML/MIN USED IN THE EXPERIMENT.
C     GM IS THE WEIGHT IN GRAMS OF THE SUBJECT TISSUE.
C     REDA IS A MEASURE OF HOW CLOSE TO AN OPTIMUM THE PARAMETERS MUST
C      BE FOR LS TO TERMINATE.  1.E-03 TO 0.E-04 IS NORMAL.  SMALLER
C      VALUES GIVE MORE PRECISION.
C     RSSTOL IS A MEASURE OF THE CROSS CORRELATION  BETWEEN PARAMETERS
C      THAT WILL BE TOLERATED BY LS BEFORE IT WILL FREEZE ONE OF THE
C      PARAMETERS.  1.E-03 TO 1.E-04 IS NORMAL.  SMALLER VALUES PERMIT
C      MORE CROSS CORRELATION.
C     READ IN PARAMETERS NOT USED IN A MODEL AS -0.
C
C
C     READ IN AND PRINT OUT DATA.

      IGOR = 0
      READ 100,IEXP,IRUN,ITRACER,FPM,GM
      FLOW = FPM*100./GM
      PRINT 200,IEXP ,IRUN,ITRACER,FPM,GM,FLOW
```

```
      READ 101, NOB, NPAR, NVAR, ITMAX, LISTS, IWT
      READ 102,(W(J),J=1,NOB)
      READ 103,RSSTOL,REDA
      DO 1 J=1,NPAR
    1 READ 104, BNDLW(J), P(J), BNDUP(J), CHMAX(J), DEL(J)
      PRINT 201
      DO 2 J=1,NOB
      READ 105, (X(J,I), I=1,NVAR)
    2 PRINT 202 ,(X(J,I), I=1,NVAR)
      READ 107,TBAR
      PRINT 106,TBAR
  106 FORMAT(*0  WITH TBAR =  *,F10.3,/,*   THE DATA IN DIMENSIONLESS FO
     *RM*)
C
C   CHANGE DATA TO DIMENSIONLESS VARIABLES.
C
      DO 3 K=1,NOB
      X(K,1) = X(K,1)/TBAR
      X(K,2) = X(K,2)*TBAR
      Y(K) = X(K,2)
      IF(IWT.EQ.0) Y(K) = 1.
      Y(K) = Y(K)*W(K)
    3 PRINT 202,(X(K,I),I=1,NVAR)
C
C   CALL OPTIMIZATION SUBROUTINE.
C
      CALL OPT(NOB,Y,NPAR,B,DEL,CHMAX,BNDLW,BNDUP,REDA,RSSTOL,ITMAX,
     *LISTS)
C
C   PRINT FINAL CALCULATED VALUES.
C   PUT IN ARRAYS FOR PLOTTING.
C
      IGOR = 1
      CALL MODEL(B,F,NOB,NPAR)
      DO 4 L=1,NPAR
    4 PRINT 203,L,P(L)
```

```
      DO 5 M = 1,NOB
      PRINT 204,X(M,1),X(M,1), G(M,2)
      G(M,1) = X(M,2)
      IX(M,1) = FACTOR*X(M,1)
    5 IX(M,2) = IX(M,1)
C
C
C   PLOT VALUES OF EXPERIMENTAL AND CALCULATED DATA POINTS.
C
      CALL PLOTTER(G,60,5,2,-NOB,10,IX,IX(NOB,1))
C
C   CALCULATE REACTOR VOLUMES USING TBAR IN SEC AND FLOW IN
C    ML/MIN/100 GMS.
C
      VP = B(1)*TBAR*FLOW/60.
      PRINT 205, VP
      TBAR = TBAR - B(1)*TBAR
      IF(B(2).LE.0.) B(2) = 1.
      IF(B(7).LE.0.) B(7) = 0.
      RTV=B(4)*B(5)*B(7)/B(3)
      T1BAR=TBAR/(B(2)*(1.0+RTV))
      V1 = T1BAR*B(2)*FLOW/60.
      IF(B(5).LE.0.) B(5) = 1.
      V1CAP = V1*B(5)
      V1EX = V1*(1.-B(5))  $  V1TANK = V1CAP/B(3)
      PRINT 206, V1, V1CAP, V1EX, V1TANK
      PRINT 998,T1BAR
  998 FORMAT(* T1BAR = *,F10.5,*   SEC*)
      IF(B(4).LE.0.) GO TO 6
      T2BAR=TBAR/((1.0-B(2))*(1.0+1.0/RTV))
      V2 = T2BAR*(1.-B(2))*FLOW/60.
      V2TANK = V2/B(4)
      PRINT 207, V2, V2TANK
      PRINT 999,T2BAR
  999 FORMAT(* T2BAR = *,F10.5,*   SEC*)
    6 CONTINUE
C
C   FORMATS....
C
  100 FORMAT(2I5,A10,2F5.1)
  101 FORMAT(I5)
  102 FORMAT(16F5.1)
  103 FORMAT(2G10.3)
  104 FORMAT(8G10.3)
  105 FORMAT(8F10.3)
  200 FORMAT(*1EXPERIMENT  *I5*-*I1*  TRACER *A10,/,* TOTAL FLOW RATE =
     G*F10.3* ML/MIN*,/,* TISSUE WEIGHT = *F10.3* GM*,/,*FLOW/100 GM = *
     GF10.3* ML/MIN/100 GM*/)
  201 FORMAT(*0  THE INPUT DATA FOLLOWS... */*0    X(J,I)...  Y(J)*)
```

```
202 FORMAT(10X,5(1PE12.5,3X))
203 FORMAT(5X,*R(*I2*) = *,F10.4)
204 FORMAT(4X,*THETA = * F6.3,5X,*E(*F6.3*) = *1PE11.4)
205 FORMAT(*0 THE PLUG FLOW REACTOR VOLUME IS * F10.3* ML/100 GM.*)
206 FORMAT(*0 CHANNEL 1 VOLUME = * F10.3, * ML/100 GM.*/,5X,*  CAPILLA
   BRY VOLUME = * F10.3,* ML/100 GM.*,/,5X,*  INTERSTITIAL SPACE VOLUM
   OE = * F10.3,* ML/100 GM.*,/,5X,*  VOLUME PER TANK IN SERIES = *
   RF10.3,* ML/100 GM.*,/,/,/)
207 FORMAT(*0 CHANNEL 2 VOLUME = * F10.3 * ML/100 GM.*/,5X,
   G *  VOLUME PER TANK IN SERIES = * F10.3* ML/100 GM.*)
    END
```

```
      FUNCTION FAC(N)
      FAC = 1
    1 IF(N.LE.0) GO TO 2
      FAC = FAC*N   $   N = N - 1
      GO TO 1
    2 CONTINUE
      RETURN
      END
```

```
      FUNCTION RFAC(X)
      DATA PI/3.141592653591
      IF(X.GT.10.) GO TO 2
      M = 11-X          $   X = X + M
     M139./51840./X**3 + 1.)
      DO 1 J=1,M
      RFAC = RFAC/X
    1 X=X-1.
      GO TO 3
    2 RFAC = SQRT(2.*PI*X)*(X**X)*EXP(-X)*(1./12./X + 1./288./X**2 -
     R 139./51840./X**3 + 1.)
    3 CONTINUE
      RETURN
      END
```

```
      SUBROUTINE SERIES(B,F,NOB,NPAR,IHOPE)
C
CC
CC    THE MODEL SUBROUTINE COMPUTES THE VALUES FOR THE ONE OR TWO STREAM
CC     NON-DIFFUSING MODELS.
CC
C
        DIMENSION B(10), F(60), TERM(4)
        COMMON/IWT/IWT



        COMMON X(60,5), G(60,5), W(60), FRAC, IGOR
        REAL N, M
        ENTRY MODEL
C
CC    B(1) IS THE RATIO OF PLUG FLOW VOLUME TO TOTAL VOLUME.  (EPS)
CC    B(2) IS THE FRACTION OF FLOW TO STREAM ONE.  (EF)
CC    B(3) IS THE NUMBER OF TANKS IN SERIES IN STREAM ONE. (N)
CC    B(4) IS THE NUMBER OF TANKS IN SERIES IN STREAM TWO. (M)
CC    B(5) IS NOT USED IN THIS MODEL.
CC    B(6) IS NOT USED IN THIS MODEL.
CC    B(7) IS THE RATIO OF VOLUMES FOR A TANK IN STREAM 2 TO A TANK IN
CC     STREAM 1, V2/V1.  (ETA)
CCC
CC    EVALUATE CONSTANTS.
CC
        EPS = B(1)   $  EF = B(2)   $  N = B(3)
        M = B(4)     $   ETA = B(7)    $   B(5) = 1.0
        ALPHA = 1.      $    BETA = 1.
        IF(ETA.EQ.0.0) EF=1.0
        CHECK = 1.-EF
        IF(CHECK.LT.1.E-10) GO TO 3
        ALPHA = ETA*M/N*EF/(1.-EF)
        BETA = EF + (1.-EF)*ALPHA
      3 CONTINUE
C
CC    CALCULATE THE MODEL VALUES.
CC
        DO 10 J=1,NOB
        THETA = (X(J,1) - EPS)/(1. - EPS)
        IF(THETA.LT.0.00)THETA=0.0
        TERM(1) = EF*((N*BETA)**N)/RFAC(N-1)*(THETA**(N-1))*EXP(-N*BETA*
     BTHETA)/(1.-EPS)
        TERM(2) = (1.-EF)*((M*BETA/ALPHA)**M)/RFAC(M-1)*(THETA**(M-1))*EXP
     0(-M*BETA*THETA/ALPHA)/(1.-EPS)
        F(J)=TERM(1) + TERM(2)
C
CC    SAVE THE CALCULATED VALUES FOR PLOTTING.
CC
        G(J,2) = F(J)
```

```
C
CC    NORMALIZE ESTIMATES IF IWT EQUALS ZERO.
C
        IF(IWT.EQ.0) F(J)=F(J)/X(J,2)
C
CC    WEIGHT EACH DATA POINT.
C
        F(J)=F(J)*W(J)
        IF(IGOR.EQ.0) GO TO 10
C
CC    CALCULATE THE TRACER RECOVERED AT THE LAST CALCULATED POINT.
C
        IN = N   $   Z1 = N-IN   $   IF(ABS(Z1).GT..5)  IN = IN+1
        IM = M   $   Z2 = M-IM   $   IF(ABS(Z2).GT..5) IM = IM + 1
        IF(IN.EQ.1) GO TO 15
        GO TO 16
   15   PROD=BETA*THETA+1.
        GO TO 17
   16   CONTINUE
        NP  = IN-1   $   PROD = 1.
        DO 1 I=1,NP
    1   PROD = PROD*BETA*IN*THETA/(IN-I) + 1.
   17   CONTINUE
        T1 = EF*(-EXP(-IN*BETA*THETA)*PROD + 1.)
        IF(IM.EQ.1) GO TO 18
        GO TO 19
   18   PROD=BETA*THETA/ALPHA+1.
        GO TO 20
   19   CONTINUE
        MP  = IM- 1   $   PROD = 1.
        DO 2 I=1,MP
    2   PROD = PROD*BETA*IM*THETA/ALPHA/(IM-I) + 1.
   20   CONTINUE
        T2 = (1.-EF)*(-EXP(-IM*BETA*THETA/ALPHA)*PROD + 1.)
        FRAC = T1 + T2
   10   CONTINUE
        RETURN
        END
```

```
      SUBROUTINE FRIEDMN(B,F,NOB,NPAR)
C
CC
CC    THE MODEL SUBROUTINE COMPUTES THE PREDICTED VALUES OF THE TWO
CC     CHANNEL DIFFUSIBLE MODEL PROPOSED BY FRIEDMAN.
CC
C
C
C
C
      DIMENSION B(10),F(60), TERM(4), R(2),CAY(2)
      COMMON/IWT/IWT
      COMMON X(60,5), G(60,5), W(60), FRAC, IGOR
      ENTRY MODEL
C
CC    B(1) IS THE RATIO OF PLUG FLOW VOLUME TO TOTAL VOLUME.  (EPS)
CC    B(2) IS THE FRACTION OF FLOW TO STREAM ONE.  (EF)
CC    B(3) IS THE NUMBER OF TANKS IN SERIES IN STREAM ONE. (N)
CC    B(4) IS THE NUMBER OF TANKS IN SERIES IN STREAM TWO. (M)
CC    B(5) IS THE FRACTION OF THE EFFECTIVE VOLUME OF THE EXCHANGE CHANNEL
CC     THAT IS LOCATED IN THE CAPILLARIES.  (GAMMA)
CC    B(6) IS THE RATIO OF FLOW BETWEEN EXCHANGE TANKS TO THE MAIN STREAM FLOW.
CC     FLOW. (D)
CC    B(7) IS THE RATIO OF VOLUMES FOR A TANK IN STREAM 2 TO A TANK IN
CC     STREAM 1, V2/V1.  (ETA)
CC
CC    EVALUATE CONSTANTS.
C
      EPS = B(1)  $  EF = B(2)  $ AN = B(3)
      AM= B(4)  $  GAMMA = B(5)  $  D = B(6)  $  ETA = B(7)
      M=AM   $  Z=AM-M  $ IF(ABS(Z).GT..5) M=M+1
      N=AN   $  Z=AN-N  $ IF(ABS(Z).GT..5) N=N+1
      ALPHA = ETA*M*EF*GAMMA/N/(1.-EF)
      A = GAMMA/(N + GAMMA - N*GAMMA)
      BETA = EF + (1.-EF)*ALPHA
      BET = EF + (1.-EF)*ALPHA/GAMMA
      EPS = EPS*BET/(BETA - EPS*BETA + EPS*BET)
      R(1)=(1.-A+D)/2./A/(1.-A)*(-1.+SQRT(1.-4.*A*D*(1.-A)/(1.-A+D)**2))
      R(2)=(1.-A+D)/2./A/(1.-A)*(-1.-SQRT(1.-4.*A*D*(1.-A)/(1.-A+D)**2))
      Q= (A*N + 1.-A)/A
      CAY(1) = (R(1)+D/(1.-A))/(R(2)-R(1))/(1.+A*R(1))**(N-1)
      CAY(2) = (R(2)+D/(1.-A))/(R(2)-R(1))/(1.+A*R(2))**(N-1)
C
C     CALCULATE THE MODEL VALUES.
      DO 10 J=1,NOB
      THETA = (X(J,1) - EPS)/(1. - EPS)
      IF(THETA.LT.0.00) THETA=0.00
      DO 2 K=1,2
      PROD=1.  $  N2=N-2
      IF(N.LE.2) GO TO 2
      DO 1 KK=1,N2
    1 PROD=PROD*(Q*BETA*(1.+A   *R(K))*THETA)/(N-KK-1) +1.
```

```
     2 TERM(K)=FF*Q*BETA*CAY(K)*(EXP(-Q*BETA*THETA)*PROD-EXP(Q*A
      R*R(K)*BETA*THETA))*(-1.)**(K+1)
        TERM(3)=(1.-EF)/FAC(M-1)*((M*BETA/ALPHA)**M)*(THETA**(M-1))*EXP(-M
      B *BETA/ALPHA*THETA)
        F(J) = TERM(1)/(1.-EPS) + TERM(2)/(1.-EPS) + TERM(3)/(1.-EPS)
C
CC    SAVE THE CALCULATED VALUES FOR PLOTTING.
C
        G(J,2) = F(J)
C
CC    NORMALIZE ESTIMATES IF IWT EQUALS ZERO.
C
        IF(IWT.EQ.0) F(J)=F(J)/X(J,2)
C
CC    WEIGHT EACH DATA POINT.
C
        F(J) = F(J)*W(J)
C
CC    CALCULATE THE TRACER RECOVERED AT THE LAST CALCULATED POINT.
C
        IF(IGOR.EQ.0) GO TO 10
        T1=0.   $  T2=0.
        IF(N.LE.2) GO TO 6
        DO 4 I=1,N2
        NI1= N-I-1   $  PROD=1.
        DO 3 K=1,NI1
     3 PROD=PROD*Q*BETA*THETA/(N-I-K) + 1.
        SUM=PROD + 1.
        AR1= (1. +A*R(1))**(N-I-1)
        AR2= (1. + A*R(2))**(N-I-1)
        T1 = T1 -EXP(-Q*BETA*THETA)*SUM*AR1 + AR1
     4  T2= T2 + EXP(-Q*BETA*THETA)*AR2*SUM - AR2
     6  T1= T1-EXP(-Q*BETA*THETA) + 1.
        T2= T2 + EXP(-Q*BETA*THETA) - 1.
        MP=M-1
        PROD=1.
        IF(M.LE.1) GO TO 17
        GO TO 18
    17  PROD=(M*BETA*THETA/ALPHA)+1.
        GO TO 19
    18  CONTINUE
        DO 5 K=1,MP
```

```
 5 PROD=PROD*(M*BETA*THETA/ALPHA)/(M-K) + 1.


19 CONTINUE
   T3=-EXP(-M*BETA*THETA/ALPHA)*PROD + 1.
   FRAC = EF*CAY(1)*(T1-(EXP(G*A*R(1)*BETA*THETA)-1.)/A/R(1)) +
  I EF*CAY(2)*(T2+(EXP(G*R(2)*A*BETA*THETA)-1.)/A/R(2)) + (1.-EF)*T3
10 CONTINUE
   RETURN
   END
```

BIBLIOGRAPHY

BIBLIOGRAPHY

1. Baker, C. H. "Blood Flow and Volume Distribution with Elevated Venous Pressure." American Journal of Physiology, 218(3):674-680 (March, 1970).

2. Baker, C. H., and Menninger, R. P. "Histamine-induced Peripheral Volume and Flow Changes." American Journal of Physiology, 226(3):731-737 (March, 1974).

3. Baker, C. H., and Davis, D. L. "Isolated Skeletal Muscle Blood Flow and Volume Changes during Contractile Activity." Blood Vessels, 11:32-44 (1974).

4. Baker, C. H.: Menninger, R. P.: Schoen, R. E.; and Sutton, E. T. "Skeletal Muscle Vascular Volume Changes with Increased Venous Pressure." Blood Vessels, 13:222-237 (1976).

5. Bischoff, K. B., and Dedrick, R. L. "Generalized Solution to Linear, Two-compartment, Open Model for Drug Distribution." Journal of Theoretical Biology, 29:63-83 (1970).

6. Borghi, M. R. "Mathematical Simulations of Isotope Extractions in Nutritional and Nonnutritional Flow Channels in Vascular Beds." Master's thesis, Michigan State University, 1976.

7. Danckwerts, P. V. "Continuous Flow Systems." Chemical Engineering Science, 2(1):1-13 (Feb., 1953.

8. Friedman, J. J. "Microvascular Flow Distribution and Rubidium Extraction." Federation Proceedings, 24:1099-1103 (1965).

9. Friedman, J. J. "Total, Non-Nutritional, and Nutritional Blood Volume in Isolated Dog Hindlimb." American Journal of Physiology, 214(1): 151-156 (1966).

10. Friedman, J. J. "Muscle Blood Flow and ^{86}Rb Extraction: ^{86}Rb As a Capillary Flow Indicator." American Journal of Physiology, 214(3):488-493 (1968).

11. Friedman, J. J. "Single-passage Extraction of ^{86}Rb from the Circulation of Skeletal Muscle." American Journal of Physiology, 216(3):460-466 (1969).

12. Goodnight, M. L. Master's thesis, to be published, Michigan State University, 1978.

13. Hamilton, W. F.; Moore, J. W.; Kinsman, J. M.; and Spurling, R. G. "Simultaneous Determination of the Pulmonary and Systemic Circulation Times in Man and of a Figure Related to the Cardiac Output." American Journal of Physiology, 84: 338-344 (1928).

14. Hamilton, W. F.; Moore, J. W.; Kinsman, J. M.; and Spurling, R. G. "Further Analysis of the Injection Method, and of Changes in Hemodynamics Under Physiological and Pathological Conditions." American Journal of Physiology, 99:534-551 (1932).

15. Himmelblau, D. M., and Bischoff, K. B. Process Analysis and Simulation. New York: John Wiley and Sons, 1968.

16. Levenspiel, O. Chemical Reaction Engineering. New York: John Wiley and Sons, 1972.

17. Martin, P., and Yudilevich, D. "A Theory for the Quantification of Transcapillary Exchange by Tracer-dilution Curves." American Journal of Physiology, 207(1):162-168 (1964).

18. Meier, P., and Zierler, K. L. "On the Theory of the Indicator-dilution Method for Measurement of Blood Flow and Volume." Journal of Applied Physiology, 6(12):731-744 (June, 1954).

19. Moore, J. C., and Baker, C. H. "Red Cell and Albumin Flow Circuits During Skeletal Muscle Reactive Hyperemia." American Journal of Physiology, 220(5);1213-1219 (1971).

20. Mountcastle, V. B., ed. Medical Physiology. St. Louis: The C. V. Mosby Company, 1974.

21. Naor, P., and Shinnar, R. "Representation and Evaluation of Residence Time Distributions." Industrial and Engineering Chemistry, Fundamentals, 2(4):278-286 (1963).

22. Renkin, E. M. "Exchangeability of Tissue Potassium in Skeletal Muscle." American Journal of Physiology, 197(6):1211-1215 (1959).

23. Renkin, E. M. "Transport of Potassium-42 from Blood to Tissue in Isolated Mammalian Skeletal Muscles." American Journal of Physiology, 197(6):1205-1210 (1959).

24. Renkin, E. M., Hudlicka, O., and Sheehan, R. M. "Influence of Metabolic Vasodilatation on Blood-tissue Diffusion in Skeletal Muscle." American Journal of Physiology, 211(1):87-98 (1966).

25. Renkin, E. M. "Blood Flow and Transcapillary Exchange in Skeletal and Cardiac Muscle." Int. Symp. on the Coronary Circulation and Energetics of the Myocardium, Milan 1966, pp. 18-30, New York: Karger, Basel, 1967.

26. Zierler, K. L. "Circulation Time and the Theory of Indicator-dilution Methods for Determining Blood Flow and Volume." In Handbook of Physiology, Sec. 2 Circulation, Vol I., Washington, D. C., Am. Physiol. Soc., 1962.

27. Zierler, K. L., M.D. "Theory of Use of Indicators to Measure Blood Flow and Extracellular Volume and Calculation of Transcapillary Movement of Tracers." Circulation Research, 12:464-471 (May, 1963).

28. Zierler, K. L., M.D. "Equations for Measuring Blood Flow by External Monitoring of Radioisotopes." Circulation Research, 16:309-321 (April, 1965).

29. Zierler, K. L. "Tracer-dilution Techniques in the Study of Microvascular Behavior." Federation Proceedings, 24:1085-1091 (1965).